Available online at www.sciencedirect.com
SCIENCE DIRECT®
International Journal of Multiphase Flow 32 (2006) 483–498
International Journal of Multiphase Flow
www.elsevier.com/locate/ijmulflow

In search of physical parameters influenced by flow patterns in a heterogeneous two-phase mixture in microchannels using concomitant measurements

Jerry K. Keska *, William E. Simon

College of Engineering, University of Louisiana at Lafayette, 109 Devon Way, Youngsville, LA 70592, USA

Received 27 December 2003; received in revised form 14 November 2005

Abstract

Space transportation systems require high-performance thermal protection and fluid management for systems ranging from cryogenic fluid devices to primary structures, and for propulsion systems exposed to extremely high temperatures, and other space systems, e.g., integrated circuits and cooling/environment control devices for advanced space suits. Although considerable developmental effort is underway to bring promising technologies to a readiness level for practical use, new and innovative methods are still needed. One such method is the *Advanced Micro Cooling Module* (AMCM), essentially a compact two-phase heat exchanger constructed of microchannels and designed to rapidly remove large quantities of heat from critical systems by incorporating phase transition. This paper describes the results of experimental research in two-phase flow phenomena, encompassing both an experimental and an analytical approach to the incorporation of flow patterns for air–water mixtures flowing in microchannels. Specifically addressed are: (1) design and construction of a sensitive two-phase experimental system which measures both ac and dc components of in situ physical mixture parameters including spatial concentration, using concomitant methods; (2) data acquisition and analysis in the amplitude, time, and frequency domains; and (3) analysis of results including evaluation of in situ physical parameters, and assessment of their validity for application in flow pattern determination.

Keywords: Experimental data analysis; Multiphase heterogeneous mixture flow; Concomitant concentration measurements; Microchannels

1. Introduction

Although there are many different types and combinations of two-phase flows, this work deals with an adiabatic heterogeneous mixture of water and air flowing in a square submillimeter microchannel. In comparison to single-phase flow, i.e., that of water or air alone, two-phase flow is significantly different due to the presence

* Corresponding author. Tel.: +1 337 857 0835; fax: +1 337 482 6661.
E-mail address: jerrykeska@yahoo.com (J.K. Keska).

0301-9322/$ - see front matter © 2005 Elsevier Ltd. All rights reserved.
doi:10.1016/j.ijmultiphaseflow.2005.11.004

of other independent variables such as velocity of the mixture and its components, spatial concentration, film thickness, and the spatial and temporal distributions of these parameters. The effect of these additional variables creates interesting challenges in describing the flow phenomena, since these variables greatly influence the nature of the two-phase flow, resulting in significant differences in reported results, compounded by difficulty in defining the experimental conditions, in verifying and validating the measured and calculated data, and in comparing the results of different experimenters.

It is recognized today that two-phase flow in *large* channels and pipes is still scientifically one of most challenging problems to be explored since the 1940s, when Lockhart and Martinelli published a model for two-phase flow in pipes (Keska and Fernando, 1994), treating two-phase flow as a pseudo-homogenous mixture; and Duckler in the 1960s and Govier in the 1950s through 1970s recognized the significance of flow patterns for large pipes and introduced the concept of a flow pattern map based on superficial parameters, principally velocity (Vance and Lahey, 1982). This approach is still being used today; however, more and more experimenters are using in situ parameters in their investigations. Using X-ray measurement techniques for void fraction/concentration determination, Zuber and Jones in the 1960s and 1970s measured concentration fluctuations using statistical analysis (Vance and Lahey, 1982) and analyzed concentration signals in the time and frequency domains for steady-state conditions, detecting different images for various flow patterns which they identified visually. In the 1970s, other methods of concentration measurement were developed by many researchers, including a capacitive densitometer and a flow pattern detector introduced in patents by Keska et al. between 1973 and 1977 (Keska and Fernando, 1994). These innovations increased the spectrum of tools available to two-phase flow investigators in this predominantly experimental two-phase research field, and they made possible further progress in this complex endeavor, not only for large pipes, but also several years later for two-phase flow in minichannels and microchannels. By measuring the fluctuation of in situ concentration in air–water mixture flows in small channels using their own unique measurement systems, Vance and Lahey (1982) suggested a derivative of PDF as an objective flow regime indicator, while retaining other superficial parameters as flow determinants. Using in situ parameters, viz., concentration, film thickness and velocity, Keska et al. (Keska and Fernando, 1994) reported attempts at incorporating flow patterns into a phenomenological two-phase flow model, including definition of the flow pattern coefficient (Keska and Miller, 1998; Keska and Smith, 1998) with application to micro heat exchangers using two-phase flow in microchannels. Subsequently for minichannels, attempts at comparing signals for measurements of concentration, pressure, and optical noise signals using a built-in sensor cluster, were presented in (Keska and Miller, 1998; Keska and Smith, 1998) and (Keska and Williams, 1999; Keska et al., 1999). An extension of this work in application to microchannels, based on measurement of these parameters in the same time and space and comparing the results obtained for various flow patterns, is the subject of this paper.

Keska and Miller (1998), Keska and Smith (1998), proposed an advanced micro cooling module (AMCM) with two-phase forced convection and phase transition as an effective cooling mechanism to accommodate the high heat fluxes encountered in various applications such as micro-electronic packages, compact fission and fusion reactor cooling systems, micro heat exchangers for space power and propulsion thermal control, and space suit thermal control for a backpack power source such as a fuel cell. To design, analyze and control such a system, it is necessary to first develop an experimental database for the two-phase flow regimes, and for void fraction and two-phase pressure drop in microchannels.

The objective of this paper is to report the results of experimental investigations on the sensitivity of dependent, measurable, in situ parameters such as concentration, pressure, and optical signal dispersion, for various two-phase flow patterns/regimes in air–water heterogeneous mixture flows in microchannels. Experiments were conducted in transparent square microchannels (996 μm × 996 μm). A high-speed micro-camera was utilized to visually observe the two-phase flow regimes at various mixtures flow conditions, which vary from zero concentration for gas-only flow to 1.0 for water-only over the full range of concentration.

This paper also reports the results, with their validation, of an experimental investigation using two concomitant (capacitive and conductive) in situ concentration measurement methods in a horizontal air-mixture two-phase flow loop in microchannels, including documentation of concomitancy between the capacitive and conductive method of in situ concentration measurements by analysis of the data in the time, amplitude and frequency domains.

2. Related work

Most of the work by others in this area for various channel geometries is necessarily experimental, with some analytical correlations developed from the empirical data. Most commonly, data is obtained for air–water mixtures, with some experiments using refrigerants, boiling water, or an air–nitrogen mixture. Some single-phase correlations have also been attempted.

Several teams of investigators have performed experimental work on air–water mixtures using small vertical tubes of various geometries. Zhao and Bi (2001a,b) developed correlations for predicting pressure drops in single-phase laminar and turbulent flow in miniature equilateral triangular channels (hydraulic diameters ranging from 0.866 mm to 2.886 mm) using high-speed video recorders (up to 12,000 pictures per second split-screen) and dynamic pressure drop measurements; they compared flow regime transition boundaries for the triangular microchannels to experimental data for small round tubes and square channels. In these experiments, four physical parameters were measured: water flow rate, air flow rate, absolute pressure and pressure drop; air and water superficial velocities were also obtained. Shuai et al. (Shuai et al., 2003) investigated flow boiling of water in small rectangular channels (hydraulic diameters 0.8 and 2.67 mm) using a video camera to investigate transition of the flow pattern and to generate preliminary flow pattern maps. Measured parameters included mass flow rate, input heating power, inlet and outlet temperature, wall temperature, and pressure drop between the inlet and outlet of the test section. Kandlikar (2002) conducted a comprehensive review of literature on evaporation in small-diameter passages (circular, rectangular, triangular and annular, with characteristic dimensions of 0.035–6.0 mm), including experiments he had performed earlier for water evaporating in small-hydraulic-diameter (1 mm × 1 mm square) multichannel passages.

Other experimental investigations were conducted using air–water mixtures flowing in small horizontal tubes of different geometries. Triplett et al. (1999a,b) performed visual observations of gas–liquid two-phase flow patterns in long circular microchannels (1.1 and 1.45 mm diameter) and semi-triangular tubes (triangular with one corner smoothed, hydraulic diameters 1.09 and 1.49 mm), obtaining two-phase pressure drop measurements, and developing void fraction experimental estimates from the photographs. Using high-speed video techniques, Coleman and Garimella (1999) developed flow regime maps and investigated transition regions for air–water two-phase flow in round and rectangular tubes with hydraulic diameters from 1.3 to 5.5 mm, for gas and liquid superficial velocities ranging from 0.1 to 100 m/s and 0.01 to 10.0 m/s, respectively. They concluded that for tubes with diameters less than 10 mm, diameter and surface tensions effects play an important role in determining the flow patterns and transitions between them. Ewing et al. (1999) performed similar experimental studies, identifying flow regimes using visual observations and photographic data, in a small transparent circular channel (1.9 cm ID), and comparing them with predictions made by other investigators. An experimental investigation was also performed (Kawahara et al., 2002) using a mixture of de-ionized water and nitrogen gas flowing in a small horizontal circular tube (0.1 mm ID). Using pressure measurements and video recorded data, two-phase frictional pressure drop and time-averaged void fraction were obtained, and two-phase flow patterns were developed and analyzed for gas and liquid superficial velocities of 0.1–60 m/s and 0.02–4.0 m/s, respectively.

Various experimental and analytical investigations with two-phase refrigerants and refrigerants with lubricating oil have been carried out in small horizontal tubes. Wong and Ooi (1995) performed an analytical study of a homogeneous two-phase refrigerant flow in a capillary tube approximately 1 mm in diameter in which the effects of various two-phase viscosity correlations on the homogeneous flow model prediction were assessed by comparing predicted pressure drops with measured data. Wongwises et al. (2002) investigated flow patterns in refrigerants with and without lubricant oils in smooth horizontal tubes with inside diameter 7.8 mm in an insulated vapor compression refrigeration system using temperature, pressure and flow rate measurements. Using this measured data and that of a high-speed camera, they developed two-phase flow patterns for flows with mass fluxes of 150–500 kg/m^2 s for a lubricating oil concentration of 5%. Yang and Shieh (2001) conducted an experimental investigation using a refrigerant flowing in small horizontal tubes with inside diameter 1.0–3.0 mm, comparing the results to similar flows in an air–water mixture. They concluded that surface tension has a significant effect on flow pattern characteristics in small tubes.

3. Experimental program

An experimental system for investigating two-phase flow in microchannels was developed. The system consists of a flow set-up with unique measurement systems for obtaining mixture concentration using both capacitive and conductive sensors, an optical system, and pressure measurement devices, all interfaced to a computer-aided data acquisition system based on Lab VIEW and MatLab software. The experimental apparatus consists of a horizontal transparent microchannel of cross-section 996 μm × 996 μm and 105 mm in length, which is supplied by controlled air and water flow from a mixing chamber. The mixing chamber allows the air and water flows to become fully mixed before entering the test section, as shown in Figs. 1 and 2. Input and output flow rates of air and water are controlled and measured by various instruments, viz., cylinders, rotameters, and scale, time and length meters, all operating in an open-loop mode.

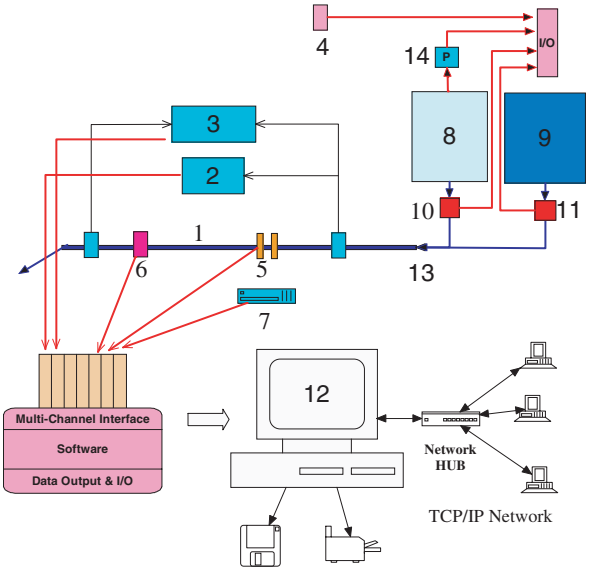

Fig. 1. Adiabatic two-phase flow system in microchannels: (1) microchannel, (2) static pressure sensor, (3) differential pressure sensor, (4) temperature sensor, (5) capacitive and conductive sensors, (6) optical sensor, (7) function generator, (8) air tank, (9) water tank, (10) air flowmeter, (11) water flowmeter, (12) Computer aided data acquisition system (CADAS), (13) air–water mixture input and (14) pressure sensor.

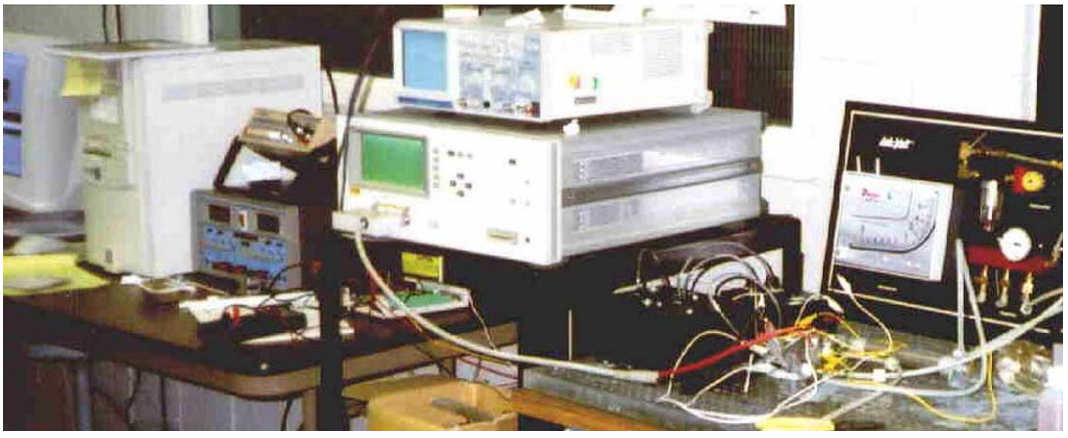

Fig. 2. Experimental system for two-phase flow in microchannels.

Within the test section, two independent and concomitant measurement systems were used to measure the in situ spatial concentration of the air–water mixture flowing through the capacitive and conductive sensors. A schematic representation of the experimental set-up is shown in Fig. 1. It is important to note that in any investigation of flow pattern phenomenon where results are based solely on visual observation, the ability of the observer and the state of the equipment often determine the quality of the results. Secondly, in most of the reported results in the literature, superficial parameters are used which have an impact on the test loop properties, thus impeding the transferability of the results to other conditions. Additionally, the bias error of the instruments used, due to the nature of the spatial and temporal distribution, may significantly impact the results. One of the objectives, therefore, of this work was to seek a solution, which would minimize those impacts. The applied solution to that problem was to place all sensors in the same location and to acquire data simultaneously for all measured parameters, providing the advantage of identical flow conditions for any given flow pattern, which eliminates the necessity of observation, or even of identifying the flow pattern occurring in the space and time of a particular measurement. If, then, for the same conditions the results are similar, and if they *remain* similar as the flow pattern changes, then concomitancy may be assumed for the measurement systems utilized.

All measurement systems, including both concentration measurements, were used to monitor the parameters of interest in the same time and space, thereby avoiding the necessity of accurately determining the flow pattern for the specifically measured conditions. Because the positioning of the sensors allowed the measurement of in situ concentration values concurrently within the same space and time, an effective comparison of concentration signals in time was obtained for all measurement systems.

In using the capacitive method of concentration measurement, the capacitance of a sensor is a function of the geometric configuration of the sensor and the dielectric constant of the mixture, which is a function of concentration for any given mixture (Keska and Fernando, 1994). This is illustrated by the following equation:

$$C = \frac{1.01\varepsilon_0 l_c}{\ln\left(1 + \frac{\pi D}{b_c}\tan h^2\left(0.7\frac{D}{b_c}\right)\right)}(\varepsilon_l c_v + (1 - c_v)\varepsilon_a) \tag{1}$$

where C is the capacitance (F), D is the channel diameter, or plate width (m), b_c is the capacitor plate width (m); ε_0 is the dielectric constant (–), ε_a is the dielectric constant of air (–), ε_l is the dielectric constant of liquid (–), l_c is the length (m), c_v the volumetric concentration (–) and h = height (m).

For concentration measurements using the conductive method, the conductance G of the sensor, made up of two plates each of area A with a distance l between the plates, and with a resistivity ρ_m between the plates and the mixture flowing between them, can be expressed by the following equation (Keska and Miller, 1998; Keska and Smith, 1998):

$$1/G = [\rho_w c_v + \rho_a(1 - c_v)]\frac{l}{A} \tag{2}$$

where G is the conductance (S), ρ_w is the density of water (kg/m^3), c_v is the air concentration (–), ρ_a, ρ_w, ρ_m are the resistivity of air, water, mixture respectively (Ω m), l is the distance between plates (m); and A the plate area (m^2).

The two concentration measurement systems consist of two electrodes opposing one another on the inside of the microchannel in a non-intrusive way, and the changes in capacitance and conductance values over time were translated into a proportional analog voltage signal and fed into the Computer Aided Data Acquisition System (CADAS).

In the calibration process for the concentration measurement systems, correlations between the capacitance and conductance of the sensor and in situ spatial concentration of the mixture were established based on previously published procedures and models (Keska and Fernando, 1994). An example of the calibration process for typical flow conditions is illustrated in Fig. 3a.

In the top row (Fig. 3a), for given and steady-state flow conditions, the conductance of the sensor is measured as a function of time at four-second time intervals, after which, by means of the calibration curve, the conductance is converted to a concentration signal over time as shown in the equation below.

$$C_v(G) = ((G_i - G_a)/(G_w - G_a)) \tag{3}$$

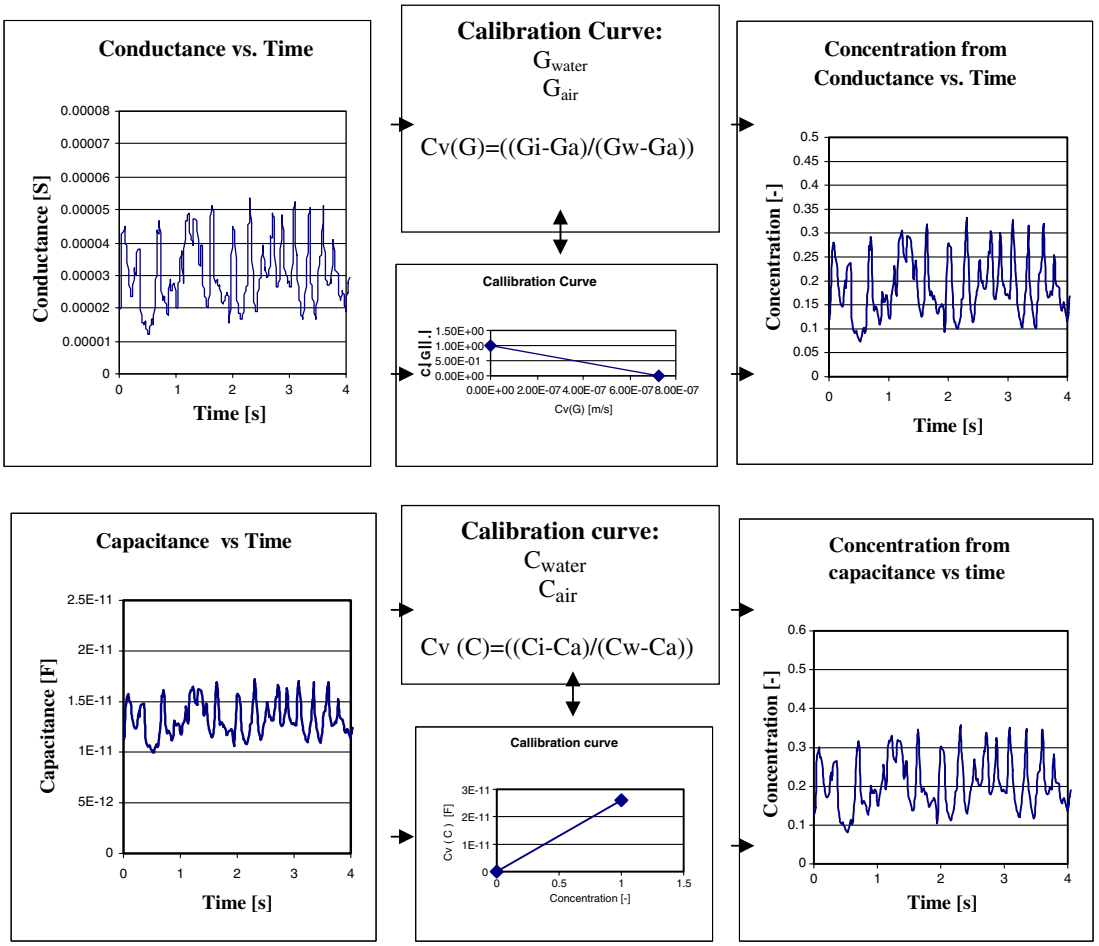

Fig. 3a. Calibration of signals from conductive and capacitive concentration measurement systems.

where C_v is the mixture in situ concentration by volume (–), G is the conductance (μS), G_i is the conductance of ith component (μS), G_a = air conductance (μS) and G_w the water conductance (μS).

Similarly, in the second row (Fig. 3a), for the same flow conditions, capacitance values of the sensor are measured as a function of time, also at four-second time intervals. Using a calibration curve, these data are converted to time-varying concentration values according to the following equation:

$$C_v(C) = ((C_i - C_a)/(C_w - C_a)) \tag{4}$$

where C is the capacitance (F), C_v is the mixture in situ concentration by volume (–), $C_v(C)$ is the mixture in situ concentration by volume from capacitive sensor (–), C_i is the capacitance of ith component (F), C_a is the capacitance of air (F) and C_w the capacitance of water (F).

Concentration measurements for both concomitant systems were obtained in identical time and space. Ideally, if the concentration values as a function of time for the conductive system are equal to the concentration values vs. time measured by the capacitive system (shown in the top and bottom rows of the last column of Fig. 3a), then both the measurement systems and the procedures used can be considered to be concomitant.

The optical sensor system consists of a light-emitting diode and a cadmium sulfide (CdS) photoresistor connected to an amplifier. The CdS cell detects the light signal passing the microchannels. Changes in light intensity caused by the interphase phenomenon deriving from the flow dynamics of the air–water mixture cause a change in cell resistance. The cell is a branch of a Wheatstone bridge, and its resistance change alters the equilibrium of the Wheatstone bridge, changing the voltage output of the bridge. These changes are magnified by

an instrument amplifier with a variable resistor connected to the negative input terminals of the two operational amplifiers, thereby controlling the amplification in a range of 100–2000×. With the CdS sensor fixed in the microchannel in close proximity to the concentration and pressure sensors, two input terminals from the instrument amplifier module are attached to the system using two Sensym ASCX series differential and static pressure sensors interfaced to the CADAS. The Lab VIEW software package is used for data gathering and analysis, system control, and various data processing tasks ranging from data filtering to digital signal processing, and data manipulation for report generation, including 3D visualizations. The frequency response of the measurement systems used is as follows: capacitive and conductive systems—140 Hz, pressure, 1 kHz; and optical system, 500 Hz. The calibration process was conducted at the start and finish of each data-gathering period using validation procedures for system hardware and software operation with standard filtering processing signals, for validation of the experimental data using the concomitancy concept.

4. Results and discussion

In order to assess the individual characteristics and change sensitivity of the various flow patterns investigated, steady-state runs were performed for all flow patterns using each of the four measurement systems (optical, pressure, conductive, and capacitive) simultaneously. Thus the data were recorded in identical time and space for the air–water mixture flow in the microchannel.

For any given steady-state condition of the flow, values of pressure, mixture transparency and concentration all fluctuate as a result of the nature of the flow and physical conditions inside the microchannel. Experimental dynamic pressure and concentration signals consist of two components, an average (dc) and a fluctuating (ac) component. The actual concentration consists of the sum of the average and fluctuating components. An example of the nature of the capacitive and conductive signals for the same time and steady-state flow conditions, measured by both systems, is presented in Fig. 3b. This example is for an average concentration of 72% with a difference between the capacitive and conductive systems of 0.7%. The top-row figures show the time traces of concentration for both the capacitive and conductive systems for a particular flow in the time domain. These traces represent the superposition of the fluctuating (ac) and time-averaged (dc) components for each signal. A visual comparison of the time traces of concentration from these two figures indicates that the signals for both systems are very similar; however, there are differences of up to 0.7% in the average values of the in situ concentration (dc components). Also, comparing visually the maximal and minimal temporal values of concentration, a strong similarity is observed in the majority of cases, although some differences are seen in the capacitive signal, where the maximum concentration is 0.50 compared to the maximum concentration value of 0.475 for the conductive signal in the same time interval. Further detailed analysis of differences in specific values, e.g., average value and signal characteristics in a given time interval, may be useful, and more detailed analysis of concentration signals in the time, amplitude and frequency domains could conceivably shed more light on the concomitancy of the measurement systems and the procedures employed.

In the next step of the analysis, from the concentration signals (top row, Fig. 3b) the average concentration values (dc component) for both systems in the same flow pattern were filtered, yielding a temporal fluctuating (ac) component of concentration in time as shown in the second row from the top, Fig. 3b. The elimination of the dc component allows for magnified visual observation of the fluctuating components of concentration vs. time. The result is a high level of similarity between the ac concentration traces of both systems.

In further expanding the depth of analysis of concomitancy and impact of the flow pattern on the signal, the ac signals are transformed into both the amplitude domain as the frequency of occurrence in function of concentration; and frequency domain as the power spectral density in function of frequency. More information about the domain analysis could be found in (Vance and Lahey, 1982), (Keska and Miller, 1998; Keska and Smith, 1998) and (Keska and Williams, 1999; Keska et al., 1999). These results are shown in the form of histograms for both the capacitive and conductive systems in the third row of Fig. 3b. Cumulative probability density functions (CPDFs) over a concentration range of −0.05–0.1 are presented in the bottom row of Fig. 3b. By analyzing the concentration range, frequency of occurrence, and the distribution shape including "skewness," taking all signals at the same flow conditions for both the capacitive and conductive systems, a

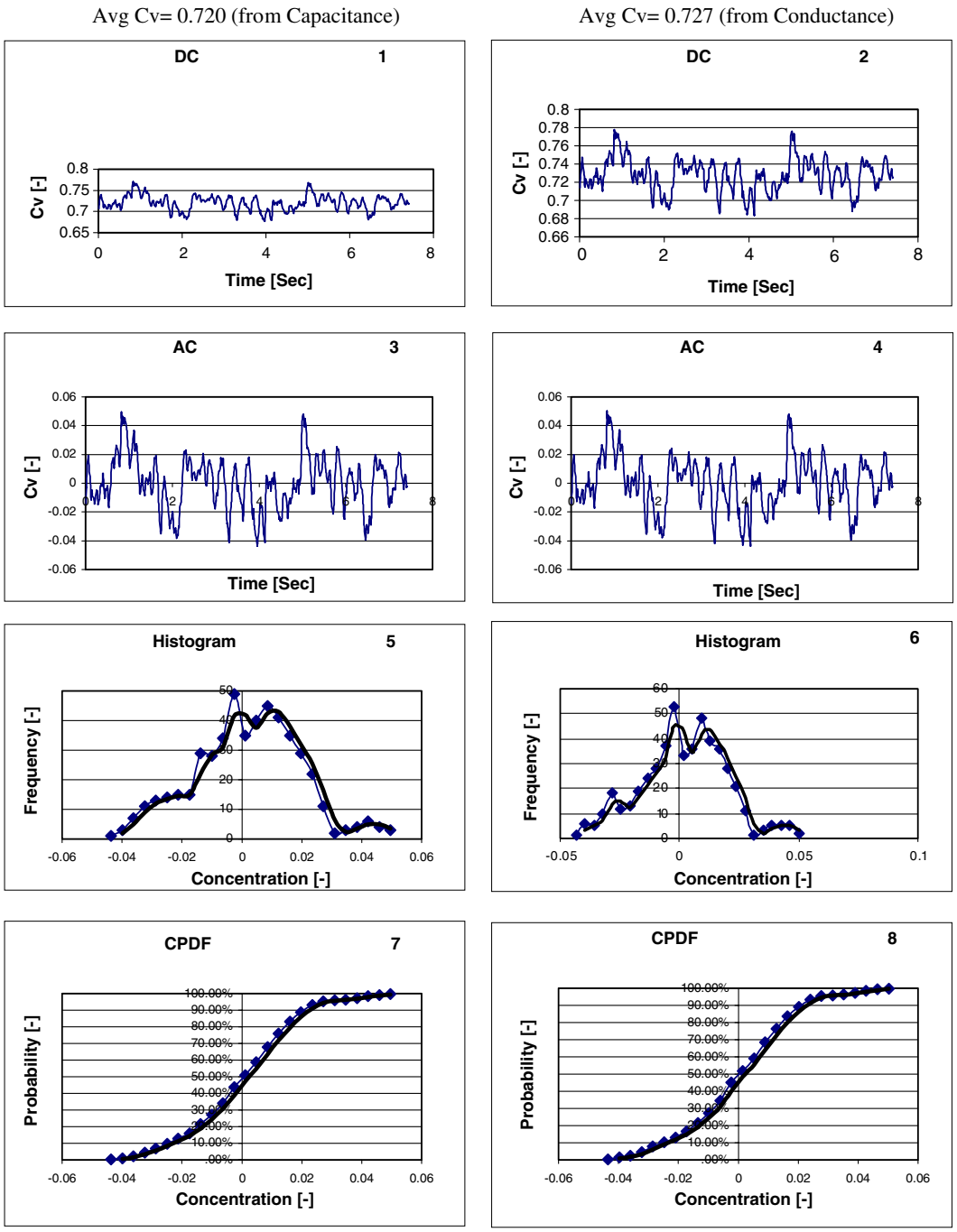

Fig. 3b. An example of in situ concentration signals from capacitive and conductive systems in time and amplitude domains.

strong similarity is noted, indicating that both the capacitive and conductive systems are concomitant with regard to concentration measurement and effects of the flow pattern for this particular experiment. In order to assess concomitancy in the entire spectrum of flow patterns, a study of such characteristics in the full range of flow pattern variation has been conducted by comparing concentration results in the time, amplitude and frequency domains for over 20 signals vs. time for evenly distributed flow pattern in the whole range of concentration from 0 to one for both capacitive and conductive systems. Due to space limitations only a few of

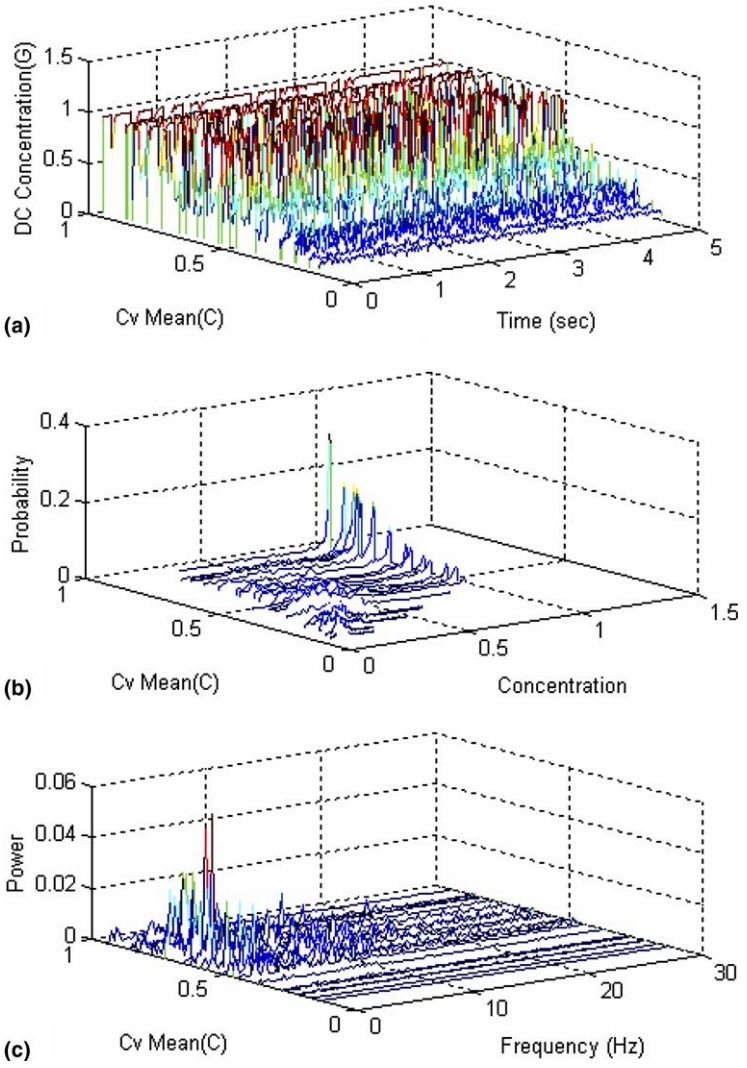

Fig. 4a. In situ spatial concentration signals in time, amplitude and frequency domains from conductive systems for air–water mixture flow in microchannels: (a) concentration from (G) with DC component, (b) PDF of concentration from (G) with DC component and (c) PSD of AC component of concentration from (G).

these measurements are presented beginning with Fig. 4a, where in the top view over 20 time traces of instantaneous concentration in 5-s time intervals for given various values of mean concentration are presented in a ''waterfall'' depiction for the conductive system. Transformation of these time traces into the amplitude domain in the middle part of Fig. 4a yields a waterfall characteristic of PDF vs. concentration for given mean values of concentration. With gradually increasing mean values of concentration from ''gas only'' to ''water only,'' it is a gradual change in dominance from all gas to pure water is noted, as distinguished by the location of the single peak. These changes occur gradually, with the all-vapor left-side peak, to two-sided peaks, and finally to the all-liquid right-side peak, for concentrations greater than 50%. In comparison to flow in large channels and minichannels, the PDF images are very similar to those obtained for microchannels. In a direct comparison of both capacitive and conductive systems, it is useful to compare characteristics for both systems as illustrated in Fig. 5a, where the PDF functions for both systems are nearly identical. Additionally, a plot of RMS values vs. concentration for both systems is illustrated in Figs. 6 and 7. These plots verify the concomitancy of both systems in terms of concentration, and their sensitivity to flow patterns.

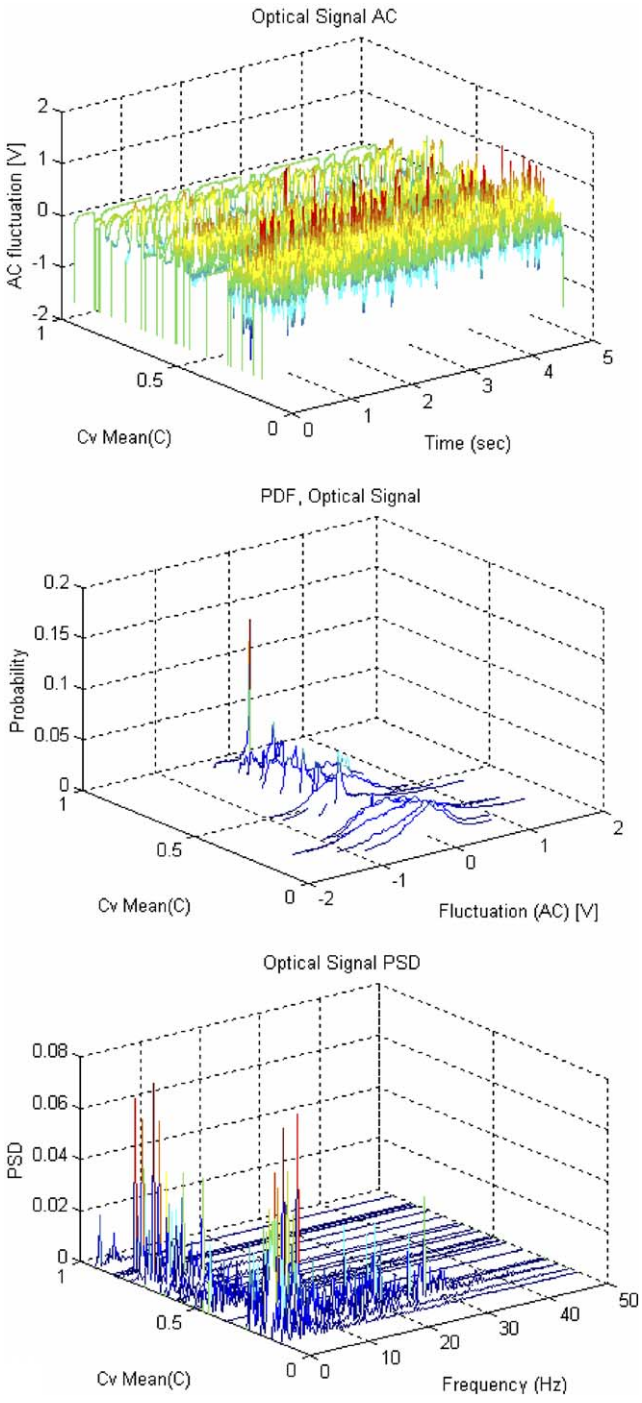

Fig. 4b. Voltage signals related to the interfacial phenomenon in the time, amplitude and frequency domains from optical systems for air–water mixture flow in microchannels.

An instantaneous value of a dynamic signal is the sum of two components: its mean value (DC) and its fluctuating (AC) component, which also can be applied for concentration, pressure, and optical signals. Figs. 4a–4c illustrate the dynamic traces of more than 20 signals in a time interval of five seconds for the entire range of concentration values between 100% gas and 100% water, in the form of "waterfall" diagrams, for concen-

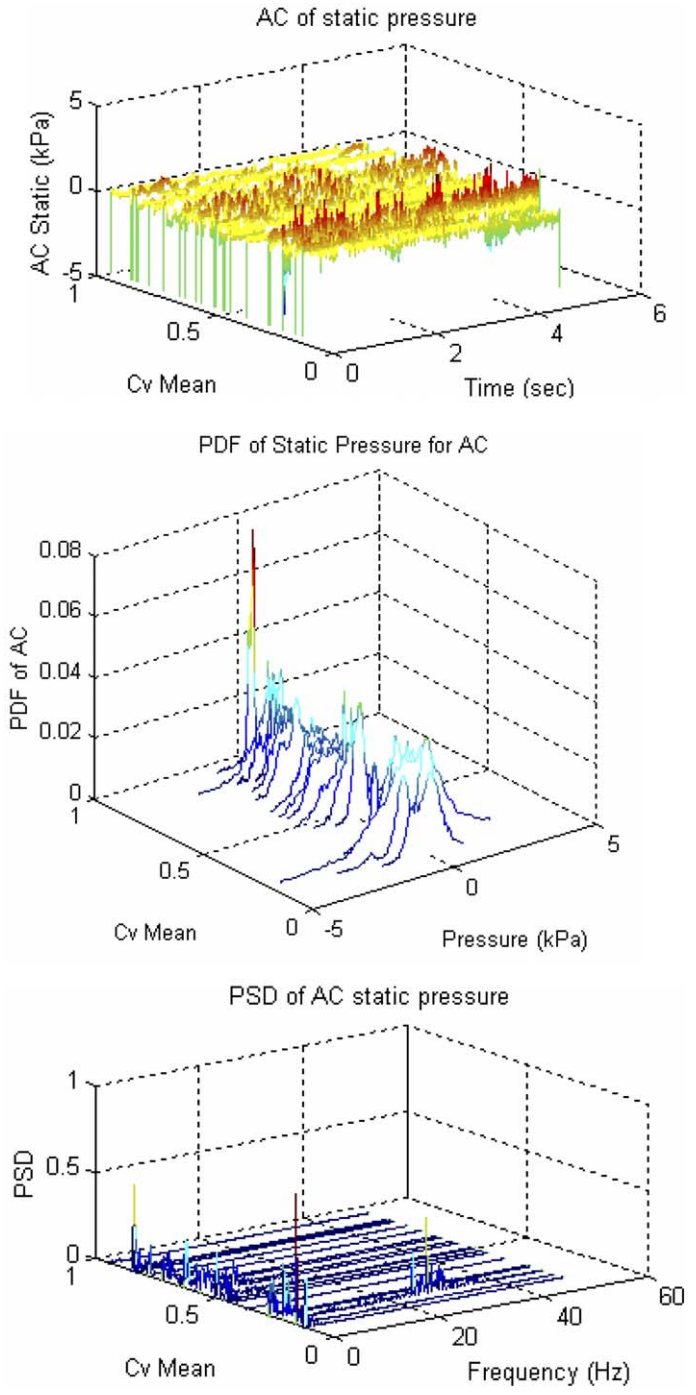

Fig. 4c. Change of probability distribution function of pressure vs. average (mean) concentration for air–water mixture flow in microchannels.

tration, optical signals and pressure, respectively. In these figures the upper frame represents a waterfall of time traces of the signals; the middle part of the waterfall represents the PDF traces, and the lower part represents the PSD of the same parameter. For example, in Fig. 5a for over 20 concentration signals in a time duration of five seconds for the entire range of concentration values between 100% gas and 100% liquid,

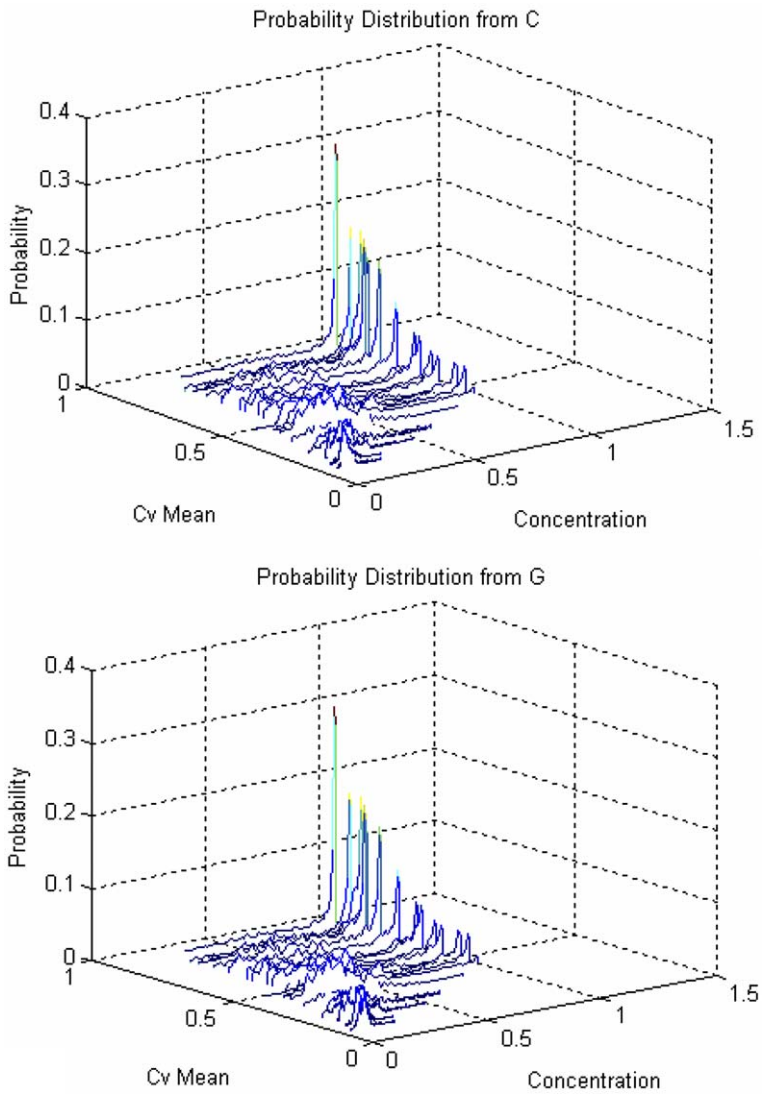

Fig. 5a. PDF functions of both in situ concentrations from capacitance and conductance sensors vs. in situ concentration from the experiments for air–water mixture flow in microchannels.

the upper chart represents the waterfall of time traces for the concentration signals, the middle part for PDF concentration after transformation of concentration signals into the amplitude domain; and the lower part illustrates PSD vs. frequency of the concentration signal after its transformation into the frequency domain. Fig. 5b shows the previously described characteristics for pressure signals. The time traces of all recorded signals are difficult to compare and correlate, but after transformation into the amplitude and frequency domains, their characteristics reveal a great deal of information concerning their structure and the characteristics of the process. Information such as range and intensity of change, frequency of change, dominant frequencies, and other characteristics of the process are readily apparent. For example, in the PDF waterfall of concentration signals (Fig. 4a), it is clearly seen on superposition of the two phenomena, that one is deterministic and the other random. This is different from the optical and pressure signals, in which both demonstrate the dominant random nature of the measurements as shown in Fig. 5b. Comparing all signals in the amplitude and frequency domains, the concentration signals alone demonstrate both deterministic and random parameters connected to the physical phenomenon, by way of the gas and water peaks in the amplitude domain.

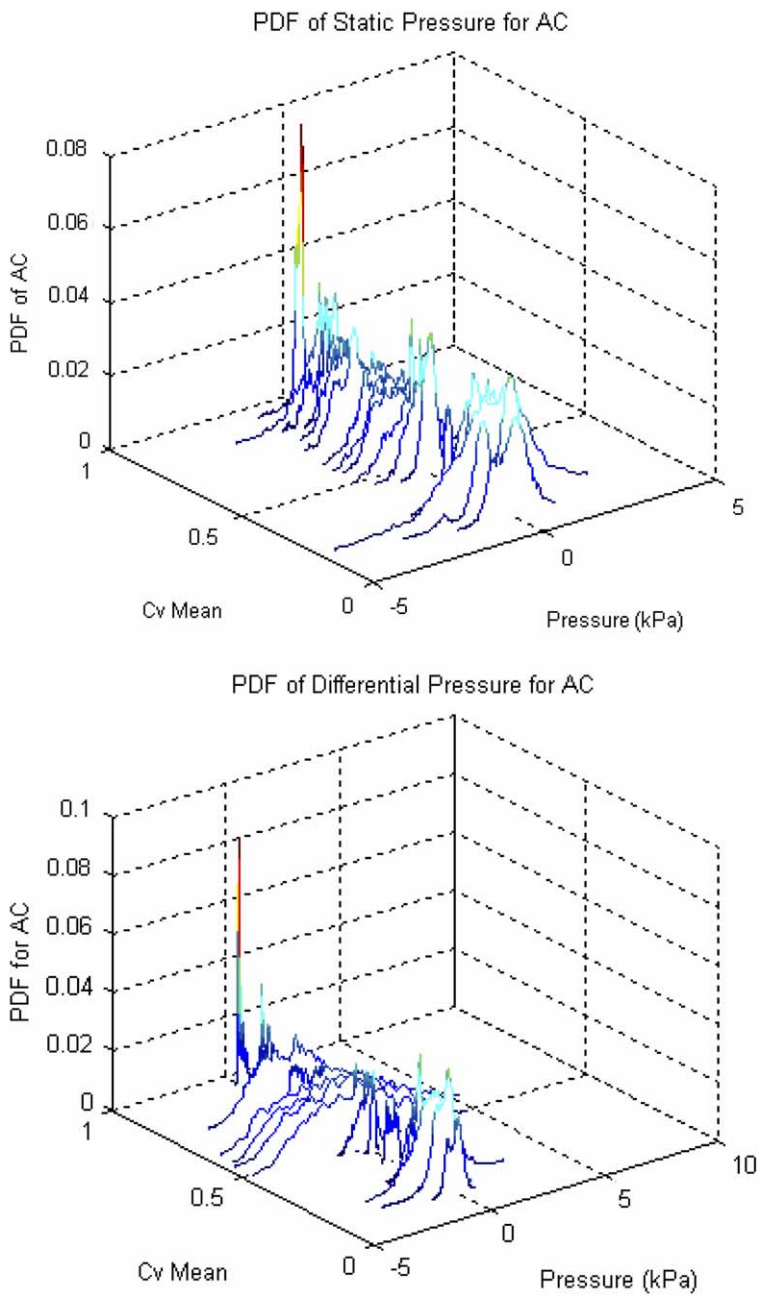

Fig. 5b. PDFs of AC components of both static and differential pressures vs. the in situ concentration from the experiments for air–water mixture flow in microchannels.

In the frequency domain, even larger differences between all signals are noticeable in terms of frequency ranges, dominant and significant frequencies, and distribution of the energy spectrum in the frequency range, which is significantly lower than the frequency response of each system. For example, the concentration and optical signal frequencies were in a similar range of 40 Hz; however, the optical signals contained many local maxima and more significant frequency than the concentration signals. The frequency range of pressure signals was in a range of single digits, which is significantly lower than that of the concentration and optical signals, with one exception in the range 20–30% concentration where the frequency range was as high as 40 Hz.

More information about the concomitancy of two concentration signals is obtained by comparing deviation of the RMS concentration values measured by both systems for the same time and space. The RMS value depends on the amplitude of the fluctuations and is given by:

$$\mathrm{RMS}_i = \sqrt{\frac{\sum(\overline{C_\mathrm{v}} - C_{\mathrm{v}i})^{\wedge}2}{N}} \tag{5}$$

where RMS_i is the root-mean square value of the signal (–), C_v is the mixture in situ concentration by volume (–), $C_{\mathrm{v}i}$ is the in situ concentration of mixture by volume of the ith component (–) and N the number of samples.

The RMS values of the in situ spatial concentration from both capacitive and conductive systems vs. in situ spatial concentration are shown in Figs. 6 and 7. As illustrated in Fig. 7, both RMS curves of concentration from the capacitive and conductive systems are very similar and the curves almost overlap.

The results of RMS values vs. in situ spatial concentration for all five-measurement systems are shown in Fig. 7, in which the RMS values are plotted against the average concentration. For comparison of each of the methods, RMS characteristics are developed with respect to average concentration, and if a "best fit" curve for the experimental points would have been drawn for each system to represent the most likely characteristics, then the steeper the curve is and the less dispersed the points are, the higher will be the sensitivity and precision

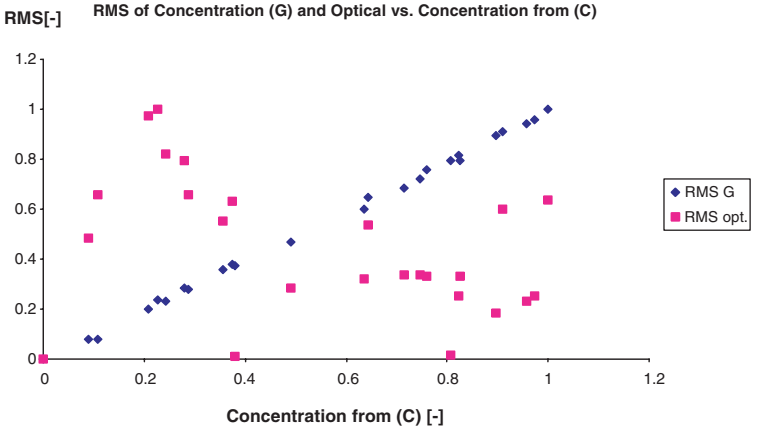

Fig. 6. RMS values of both in situ concentrations from conductance and optical signal vs. the in situ concentration from the experiments for air–water mixture flow in the microchannel.

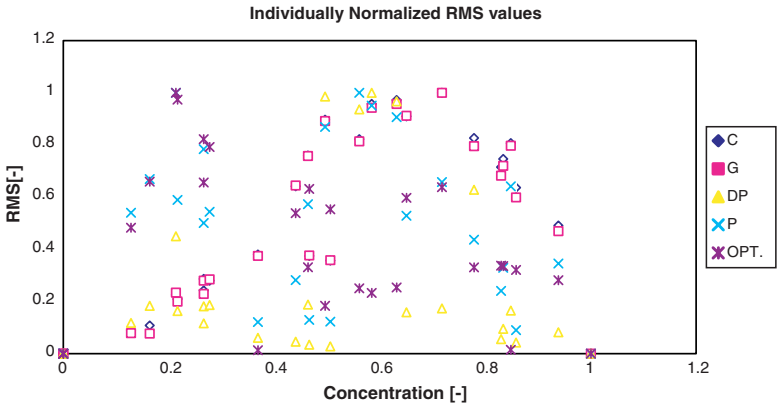

Fig. 7. Individually normalized RMS values of five parameters such as two in situ concentrations, two pressures and optical signal vs. the in situ concentration from the experiments for air–water mixture flow in microchannels.

of this system as used to define the flow pattern. For each of the systems used in the cluster, the RMS values of a signal that represents the pressures (static and differential), capacitance, conductance or optical measurement (interfacial phenomenon) of the sensor must be zero for both values of average in situ spatial concentrations of 0 or 1 (respectively for "air-only" and "water-only"), because at these two points the mixture is homogeneous and fluctuations are zero. As documented, the RMS data from the optical system has at least two local maxima, as opposed to only one maximum for the other three systems in the cluster. The maximum RMS values for the concentration signals are 0.75, for pressures around 0.65–0.70, and for optical signals 0.20 with the second local maximum around 0.75. Data points from both concentration systems are almost identical and are characterized by very small dispersions in opposition to data points for both pressure systems and optical system, which reveals that the character of the optical signal is influenced by phenomena other than pressure, and capacitive or conductive signals.

5. Conclusion

This experimental study, performed in an adiabatic microchannel system constructed to accommodate an air–water mixture flow over the full range of concentration from 0 (all water) to 1 (all gas), involved the simultaneous measurement of in situ parameters (concentration, static and differential pressures) and an optical signal related to interfacial phenomenon. For concentration measurements both capacitive and conductive concentration measurement systems were employed. Simultaneous measurement of these parameters in identical time and space under steady-state flow conditions results in the following conclusions:

(1) all measured parameters (concentration, pressure and optical signal) demonstrated sensitivity to flow patterns; however, the character and level of impact of each parameter were very diverse,
(2) both the conductive and capacitive systems of concentration measurement were found to be concomitant, with each having the same flow pattern sensitivity as demonstrated by similar "waterfalls" graphs in all domains (time, amplitude and frequency), where the concentration values measured by both systems were very similar,
(3) the RMS characteristic of the concentration measurement is suitable for use as a flow pattern determinator or measurand and
(4) pressure and optical signals demonstrated different sensitivity to flow patterns than did the concentration signals. Furthermore, the optical signals not only possess two local maxima, but they have different "max RMS" values of concentration, and they are also characterized by significant dispersion of values throughout the range of tested conditions.

Acknowledgement

The authors acknowledge support for this work from the Louisiana Board of Regents LaSpace/EPSCOR program; contract No. NASA/LEQSF (2002-04)-DART-02.

References

Coleman, J.W., Garimella, S., 1999. Characterization of two-phase flow patterns in small diameter round and rectangular tubes. Int. J. Heat Mass Transfer 42, 2869–2881.

Ewing, M.E., Weinandy, J.J., Christensen, R.N., 1999. Observations of two-phase flow patterns in a horizontal circular channel. Heat Transfer Eng. 20 (1).

Kandlikar, S.G., 2002. Two-phase flow patterns, pressure drop, and heat transfer during boiling in minichannel flow passages of compact evaporators. Heat Transfer Eng. 23, 5–23.

Kawahara, A., Chung, P.M.-Y., Kawaji, M., 2002. Investigation of two-phase flow pattern, void fraction and pressure drop in a microchannel. Int. J. Multiphase Flow 28, 1411–1435.

Keska, J.K., Fernando, R.D., 1994. Average physical parameters in an air–water two-phase flow in a small square-sectioned channel. J. Fluids Eng. 116, 247–254.

Keska, J.K., Miller, A.C., 1998. Micromechanical devices: an enhanced micro-heat exchanger for applications in high integrated microprocessors and laser diode arrays. In: Proc. of the International Mechanical Engineering Congress and Exposition (IMECE). 98-WA/EEP-19, Anaheim, CA, pp. 1–6.

Keska, J.K., Smith, M.D., Williams, B.E., 1999. Comparison study of a cluster of four dynamic flow pattern detection techniques. J. Flow Meas. Instrum. 10, 65–77.

Keska, J.K., Smith, Michael D., 1998. Statistical analysis of experimental results in amplitude and frequency domains for two-phase flow. In: Proc. of ASME Fluids Engineering Division, vol. 247. 1998, pp. 153–162.

Keska, J.K., Williams, B.E., 1999. Experimental comparison of flow pattern detection techniques for air–water mixture flow. Int. J. Exp Heat Transfer, Thermodyn Fluid Mech 19, 1–12.

Shuai, J., Kulenovic, R., Groll, M., 2003. Heat transfer and pressure drop for flow boiling of water in narrow vertical rectangular channels. In: First International Conference on Microchannels and Minichannels. ASME-ICMM2003-1084, Rochester, NY, pp. 1–7.

Triplett, K.A., Ghiaasiaan, S.M., Abdel-Khalik, S.I., Sadowski, D.L., 1999a. Gas–liquid two-phase flow in microchannels. Part I: two-phase flow patterns. Int. J. Multiphase Flow 25, 377–394.

Triplett, K.A., Ghiaasiaan, S.M., Abdel-Khalik, S.I., Sadowski, D.L., 1999b. Gas–liquid two-phase flow in microchannels. Part II: void fraction and pressure drop. Int. J. Multiphase Flow 25, 395–410.

Vance, M.A., Lahey, R.T., 1982. On the development of an objective flow regime indicator. Int. J. Multiphase Flow 8, 93–124.

Wong, T.N., Ooi, K.T., 1995. Refrigerant flow in a capillary tube: an assessment of the two-phase viscosity correlations on model prediction. Int. Commun. Heat Mass Transfer 22 (4), 595–604.

Wongwises, S., Songchang, T., Kaewon, J., Wang, Chi-Chuan, 2002. A visual study of two-phase patterns of HFC-134a and lubricant oil mixtures. J. Heat Transfer Eng. 23, 13–22.

Yang, C.-Y., Shieh, C.-C., 2001. Flow pattern of air–water and two-phase R-134a in small circular tubes. Int. J. Multiphase Flow 27, 1163–1177.

Zhao, T.S., Bi, Q.C., 2001a. Pressure drop characteristics of gas–liquid two-phase flow in vertical miniature triangular channels. Int. J. Heat Mass Transfer 44, 2523–2534.

Zhao, T.S., Bi, Q.C., 2001b. Co-current air–water two-phase flow patterns in vertical triangular microchannels. Int. J. Multiphase Flow 27, 765–782.